AIAA JOURNAL
Vol. 35, No. 4, April 1997

Impulsively Started Turbulent Jets

H. Johari,* Q. Zhang,† M. J. Rose,‡ and S. M. Bourque‡
Worcester Polytechnic Institute, Worcester, Massachusetts 01609-2280

The structure and mixing of impulsively started jets have been studied in a water tank utilizing an acid-base reaction. The flow consists of a starting vortex that separates from the rest of the jet in the near field. Penetration of the jet tip scales with the square root of time, normalized by the nozzle diameter and velocity. The celerity of the jet tip is approximately one-half of the centerline velocity of a steady jet, with the same nozzle exit velocity, at the same location. Results of chemically reactive experiments indicate that the fluid in the vicinity of the jet tip mixes with the ambient fluid faster than the rest of the jet. The extent of the region near the jet tip with improved mixing becomes larger as the jet travels further downstream. The more rapid mass mixing at the jet tip implies faster momentum diffusion, which corroborates the slowing down of the jet tip in comparison with the steady jet.

Introduction

THE steady, round turbulent jet is a flow of interest in both industrial applications and scientific inquiries. The industrial applications of the turbulent jet range from vertical/short takeoff and landing ejectors to power plant combustion chambers. Of major importance in all of these applications is the entrainment rate of the ambient fluid and the ultimate small-scale mixing of it with the injected fluid. A number of investigations have revealed that the jet near field consists of ring vortices.[1,2] These vortices form as a result of the instability of the shear layers surrounding the jet and have been the motivation for forced jet studies. The entrainment rate of fully pulsed jets has been found to be as much as twice the steady jet value.[3] However, at sufficient downstream locations, the pulsed jet characteristics reverted back to that of steady jets.

A natural extension of the steady jet flow is the impulsively started jet. Cantwell[4] studied the starting process of round jets using an axisymmetric Stokes flow approximation and obtained the particle paths at Reynolds numbers up to 30. The starting vortex becomes self-similar when the coordinates are scaled by the square root of time. The laminar starting jet was investigated by Abramovich and Solan,[5] who modeled the flow as a laminar jet combined with a spherical vortex at the tip. Their experimental data agreed with the model, and the speed of the jet tip in the far field was found to be approximately one-half of a steady jet with the same exit velocity at the same location. Kuo et al.[6] investigated the laminar starting jet by numerical methods and found a Reynolds number scaling that was different from that of Abramovich and Solan. Witze[7] also formulated the turbulent starting jet in terms of a spherical vortex attached to the jet. The laminar and turbulent starting jet models are both based on Turner's model[8] for a starting plume. Witze's model revealed that the time created by the ratio of nozzle diameter to the jet velocity is an important parameter that can correlate the results. The jet tip celerity in the turbulent case was also proportional to the centerline velocity of a steady jet (with the same exit velocity) at the same location. Using an inert tracer and image processing techniques, Lahbabi et al.[9] recently verified this proportionality in turbulent starting jets. They also showed that the starting jet entrainment, in a Lagrangian sense, was approximately 30% greater than the steady jet. Since no measurements of the small-scale mixing rate in impulsively started jets could be found in the literature, an investigation of the small-scale mixing in starting jets was undertaken.

The present effort is an experimental investigation of round, incompressible, impulsively started turbulent jets. The starting vortex and the flow immediately behind it are in unsteady motion. Our emphasis has been on the starting vortex motion, the penetration of the jet tip, and the mixing in the jet tip vicinity. The jet penetration was recorded as a function of time in a series of flow visualization experiments. Jet tip celerity was found by differentiating the penetration data with respect to time. Small-scale mixing, as revealed by a pH indicator in the presence of an acid-base neutralization reaction, was examined in starting jets.

Experimental Technique

Apparatus

The experiments were carried out in a clear acrylic water tank of 1.2×1.2 m cross section and 1.5 m depth. The jet was initiated by the sudden charging of a solenoid valve, which was supplied from a constant pressure reservoir. The solenoid valve had an opening time of about 20 ms (manufacturer's specification). The outlet of the solenoid valve was connected to a plenum and nozzle combination. The plenum contained a honeycomb section and a cross to reduce any residual swirl. Three nozzles with diameters of 0.635, 1.27, and 2.54 cm could be attached to the plenum. The contraction ratios for the three nozzles were 144, 36, and 9:1, respectively. All three nozzles had matched cubic contours to obtain nearly top-hat velocity profiles at the exit. The Reynolds number, based on the average jet velocity V_j at the nozzle exit plane and nozzle diameter d, in this setup ranged from 5×10^3 for the largest to 2×10^4 for the smallest nozzle. A schematic drawing of the setup and the flow is shown in Fig. 1; the experimental conditions, including the nozzle time d/V_j, are summarized in Table 1.

The velocity at the nozzle exit during the starting process was measured using a laser Doppler velocimetry system. Figure 2 contains time traces of the nozzle velocity for two different nozzles. At the lowest Reynolds number, the nozzle velocity underwent one oscillation cycle during the startup process. The time for the nozzle exit velocity to reach 90% of the steady-state value was found to be in the range of 10 to 50 ms for nearly all of the runs. These velocity rise times are comparable with the solenoid opening time of 20 ms.

Flow Visualization

Both ordinary and fluorescent dyes were used for tagging the jet fluid. Internal structure of the jet was revealed by the laser-induced fluorescence (LIF) technique, which utilizes a photo-sensitive dye (disodium fluorescein). The jet fluid marked with this dye fluoresced when it crossed a planar laser sheet. The light sheet was created by sweeping a laser beam back and forth at 1200 Hz. All runs were recorded on videotape, and the data were recovered once the tape was played back frame by frame. This arrangement allowed for a sampling rate of 30 Hz. Because the integration time for each frame of video (17 ms) was large compared with the laser beam oscillation period (0.8 ms), the beam was recorded as a sheet. The Kolmogorov time scale on the centerline of the steady jet was equal to the video exposure time at an axial location of $100d$. Moreover, the passage

Received June 17, 1996; revision received Dec. 13, 1996; accepted for publication Jan. 9, 1997.

*Associate Professor, Mechanical Engineering Department. Senior Member AIAA.
†Graduate Student, Mechanical Engineering Department.
‡Undergraduate Student, Mechanical Engineering Department.

Table 1 Experimental conditions

d, cm	$Re \times 10^{-3}$	d/V_j, ms
0.635	20	2.1
	12	3.4
1.27	15	10.9
	6	27.5
2.54	5	131

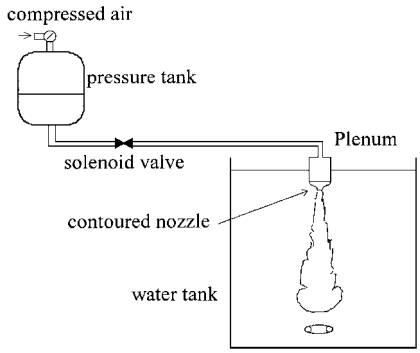

Fig. 1 Schematic of the experimental apparatus.

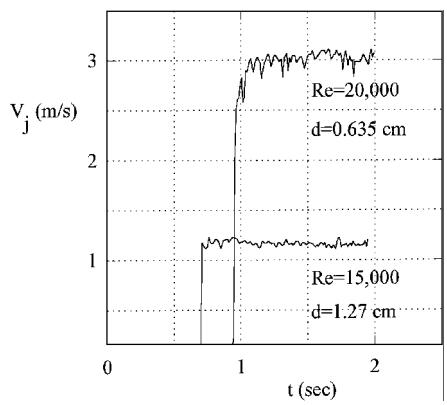

Fig. 2 Time traces of nozzle exit velocity for two cases.

time of Kolmogorov eddies on the jet centerline was much smaller than the video exposure time. Hence the images in the present study are not time resolved; however, the exposure time was much smaller than the time associated with the jet large-scale motions. Therefore, the current LIF method is adequate for examination of the large-scale features of the impulsively started jet.

The data extracted from the videotaped images were limited to the axial location of the jet tip as a function of time, with the exception of starting vortex measurements where the diameter of the vortex core was also recorded. The jet tip was clearly discernible in the LIF images because the interface between the jet and ambient fluids was distinct. This interface was highly contorted because of the small-scale eddies. Even though the interface appearance varied among different runs, the axial location of the jet tip interface was quite repeatable. The uncertainty in the axial location of the jet tip stems primarily from the inaccuracies associated with visually measuring the interface location from the video monitor.

Chemically Reactive Runs

To probe the small-scale mixing within the jet, an (isothermal) aqueous acid-base neutralization was utilized. In this set of runs, the flow was visualized by a pH indicator, phenolphthalein, which had a purplish red color in alkaline solution. The jet fluid contained the alkaline solution plus the pH indicator, whereas the tank fluid was acidic. Upon mixing with the tank fluid to a prescribed volumetric ratio ϕ, the jet fluid discolored completely. Here, ϕ is the reaction equivalence ratio, the ratio of acidic solution required to neutralize a unit of the alkaline solution. By varying the relative concentrations of the alkaline (jet) and acidic (tank) solutions, ϕ was altered. The solution concentrations were chosen to create a sharp color transition once the mixture ratio was equal to ϕ. By recording the location of the last jet parcel to discolor (i.e., molecularly mix with the ambient fluid), the minimum jet mixing rate can be determined. In other words, all of the jet parcels are molecularly mixed to at least the prescribed equivalence ratio at the location of discoloration.

The distance from the nozzle exit to the point where all the jet fluid parcels were discolored will be referred to as the reaction length of the jet. Beyond this distance, every jet parcel was mixed to at least ϕ parts of ambient fluid. The reaction length is analogous to the flame length of burning jets, especially because the reacting jets in the present experiments visually resembled burning fuel jets. The reaction length is directly related to the minimum mixing rate. At any given equivalence ratio and Reynolds number, a shorter reaction length implies increased mixing. This chemically reactive technique has been used previously to investigate molecular scale mixing in steady turbulent jets[10,11] and shear layers.[12] Reaction length was measured for a number of equivalence ratios. The reaction length of the steady jet scales with the nozzle (momentum) diameter and is independent of the Reynolds number for Reynolds numbers greater than 3×10^3 (Ref. 11). It is expected that the reaction length of the starting jet will also scale with the nozzle diameter. Furthermore, Reynolds number effects are anticipated to be small for the range of Reynolds numbers in this study.

In steady jets, the reaction length fluctuates quasiperiodically about a mean value with an oscillation period equivalent to the local jet width divided by the local mean velocity.[11] Because the impulsively started jet is an unsteady flow, the reaction length varied with time prior to settling into a stable mean at the steady jet value. The time evolution of the reaction length was measured at three equivalence ratios for each nozzle diameter. The equivalence ratios in the present study ranged from 1.3 to 9.5.

Results

Starting Vortex

As the flow was initiated impulsively, a vortex ring was created in the vicinity of the nozzle exit. The jet followed this starting vortex. The size of the vortex ring was determined primarily by the nozzle diameter. After a short time, the starting vortex ring separated from the rest of the jet. Images of the separated vortex and the jet, as revealed by a planar laser sheet containing the jet axis, are shown in Fig. 3 for the 1.27-cm nozzle. The two bright circles are the cross sections of the starting vortex core. The vortex ring proceeded with a faster velocity than the jet tip and the distance between the two increased with time (see Fig. 3). The much greater entrainment rate of the turbulent jet as compared with the vortex ring caused the jet to slow down by sharing its momentum with a larger volume of ambient fluid, whereas the core of the vortex ring remained relatively unmixed. The convective velocity discrepancy between the vortex and the jet tip caused the increasing separation between the jet and vortex ring.

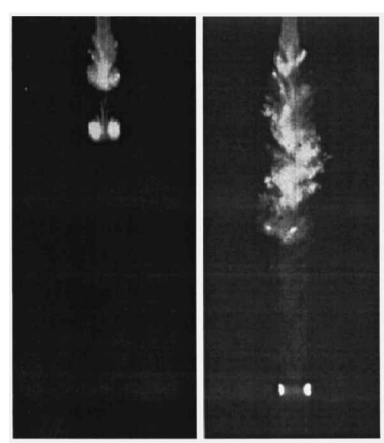

Fig. 3 Laser-induced fluorescence images of an impulsively started jet; d = 1.27 cm and $Re = 1.5 \times 10^4$. The starting vortex has just separated from the jet tip in the left-hand image. The vortex travels faster than the jet tip, as shown by the right-hand image.

The penetration and width of the vortex cores were measured from the videotape. Each video frame was analyzed visually for the axial location of vortex core and the separation distance between the centers of the two imaged vortex core cross sections, as in Fig. 3. The estimated uncertainties of ± 1.5 cm for the axial location of vortex core and ± 0.3 cm for the vortex core diameter are a result of the errors associated with the precise location of the dyed core centers and the resolution limitations of video recording. The spreading rate dr/dx of the starting vortex ring was found by fitting a straight line to the vortex radius vs axial position data because the growth of vortex core radius r was linear with axial distance. The spreading rates ranged from 0.006 to 0.014 (± 0.001), in agreement with Maxworthy's data.[13] There appeared to be no direct relation between the nozzle diameter or Reynolds number and the spreading rate of the starting vortex. We do not suspect that the details of the impulsive start play an important role in the formation of the vortex ring. This inference is based on the experiments on the formation of vortex rings in the wake of accelerating plates (normal to the freestream)[14] and on the evolution of dynamic stall vortex on airfoils undergoing pitch-up at nominally constant rate.[15] In both of these investigations the initial acceleration rate leading to either the constant velocity in Ref. 14 or the constant pitch rate in Ref. 15 did not affect the overall flow features, which evolved in time.

The vortex ring separation was observed for all nozzle diameters and Reynolds numbers. It is surprising that the previously mentioned investigations of the starting jets have not reported this phenomenon. The only references found in the literature that point to the separation of the jet starting vortex ring are Gharib et al.[16] and Kouros et al.[17] These investigations observed the separation of the starting vortex in a piston-driven setup simulating pulsatile flow through the mitral heart valve and from an unsteady starting turbulent jet using a gravity-driven setup, respectively. Although it is possible that the separation of the starting vortex may be facility dependent, three different setups in which the flows were pressure driven (present experiments), piston driven,[16] and gravity driven[17] have all resulted in the same observation at Reynolds numbers ranging from a few thousand[16] to 5×10^4 (Ref. 17). The nature of flow diagnostics is believed to have been the difference between the latter studies and the former ones, which do not report the vortex separation. The separation is most discernible when the entire flowfield within a two-dimensional cross section is examined at one instant. This was accomplished by recording the scalar field via the LIF technique in the current experiments as well as those in Ref. 17 or by measuring the velocity field by the particle imaging velocimetry technique utilized in Ref. 16. It is possible that single point measurements, as utilized by Witze[7] and Abramovich and Solan,[5] of the centerline velocity may not reveal the separation because the passage of the starting vortex would appear as a spike, well ahead of the jet tip, in the velocity time traces. The spike can be quite narrow at high Reynolds numbers, due to the rapid passage of the starting vortex, and consequently may be filtered out or averaged out (if a number of runs are ensemble averaged). Thus, the separation of the starting vortex from the jet body is proposed as an integral part of starting jets.

The time τ from the onset of the flow to the vortex separation was measured from the video images, and it depends on the nozzle diameter and the jet velocity. The separation time, defined as the time of the first image with pure ambient fluid between the starting vortex and the ensuing jet, is plotted against the nozzle time d/V_j in Fig. 4. The uncertainty in these time measurements is ± 33 ms, and it stems from the video frame not being synchronized with the startup and the separation processes. Each data point is an average of 10 runs, and the bars around each data point indicate ± 1 standard deviation for the data set. For the three lowest nozzle times, the repeatability was such that the variation between the runs was less than the symbol size on the plot. The vortex separation time appears to be nearly constant for nozzle times of less than 10 ms and increases for larger nozzle times. Gharib et al.[16] report that they found the vortex separation time, normalized by the nozzle diameter and the running-average velocity

$$\bar{V} = t^{-1} \int_0^t V_j \, \mathrm{d}t$$

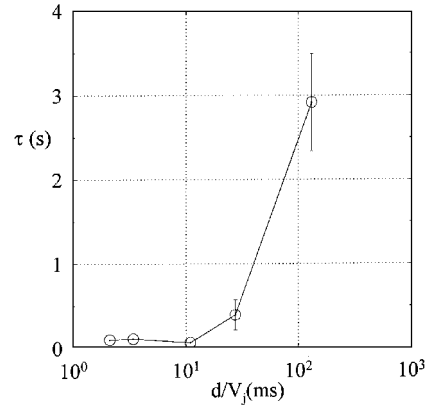

Fig. 4 Dependence of starting vortex separation time τ on nozzle time d/V_j.

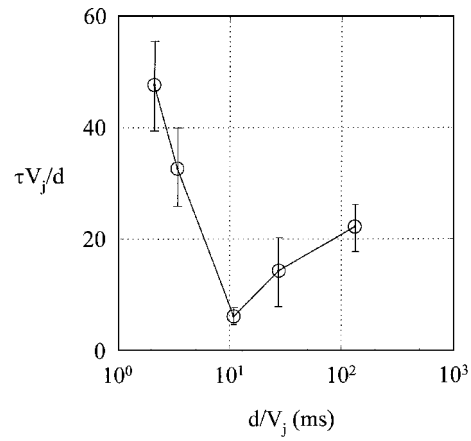

Fig. 5 Normalized vortex separation time vs nozzle time.

at the time of separation, was constant with a value of about 4. For an impulsively started flow, the running-average velocity $\bar{V}$ is the same as V_j. The present averaged vortex separation times were normalized by the nozzle time and are plotted against d/V_j in Fig. 5.

The normalized separation time in our experiments ranged from 6.1 to 47.7, in excess of the value quoted by Gharib et al.[16] The vortex separation time in the experiments of Kouros et al.,[17] when normalized by the running-average velocity $\bar{V}$ in their apparatus, yields a value of 32.3 at an average Reynolds number of 3.5×10^4. Our normalized separation time data do not appear to correlate with the nozzle time. For nozzle times less than 10 ms, the normalized separation time is expected to decrease because τ was nearly constant. For larger nozzle times, the normalized separation time increased. It was thought that τ might scale with the rise time of the velocity at the nozzle exit. However, when the vortex separation time was normalized by the average rise time associated with the specific jet exit conditions, the resulting normalized separation time still varied significantly among different cases. A proper time scale for nondimensionalizing the starting vortex separation time has not yet been found.

Jet Tip Penetration

The flow succeeding the starting vortex appeared similar to a steady jet with the large structures discernible in the jet far field. The spreading rate of the jet was independent of the nozzle diameter and the Reynolds number, consistent with previous observations.[18] The position of the jet tip X subsequent to the separation of the starting vortex was extracted from the video images and was normalized with the nozzle diameter. In all cases, the normalized jet tip position X/d increased as the square root of nondimensional time tV_j/d. This was expected from the previous measurements of Witze[7] and Lahbabi et al.[9] and can be readily derived by writing the jet centerline velocity, which is inversely proportional to the axial distance, as $\mathrm{d}X/\mathrm{d}t$. Integration with respect to time reveals that the jet tip evolves

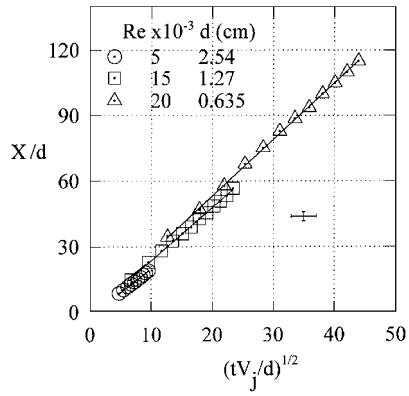

Fig. 6 Jet tip penetration for three nozzle diameters; a least-squares line is fitted to each data set.

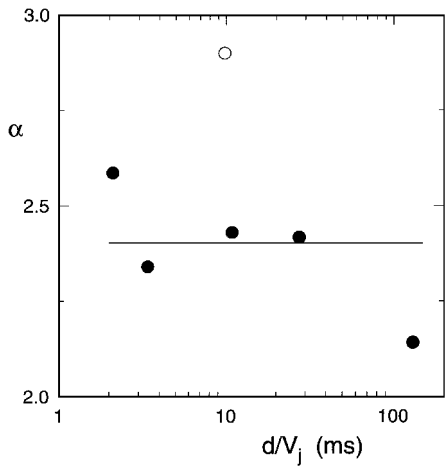

Fig. 7 Dependence of α on nozzle time. The data point denoted by the symbol ○ is from Ref. 8.

as the square root of time. Penetration as a function of square root of normalized time is shown in Fig. 6 for three nozzle diameters and Reynolds numbers. Each data set is the average of three runs; the uncertainty in jet tip position is ±1.5 cm and ±33 ms in time.

Each data set was fitted by a least-squares line representing

$$(X - X_0)/d = \alpha(tV_j/d)^{\frac{1}{2}} \tag{1}$$

The virtual origin effects were minimal since X_0/d varied between −1.6 and 1.5. The values of α ranged from 2.14 to 2.58 with an average of 2.4 for all the runs. This is to be contrasted against the value obtained by Lahbabi et al.[9] of 2.9 at a Reynolds number of 2.6×10^3. To examine whether α depends on the nozzle time, as predicted by Witze's model, α was plotted against the nozzle time in Fig. 7. There appears to be a slight reduction in α with increasing nozzle times. Because the variations of α are relatively small in the current experiments, i.e., are within 10% of the mean value, we will assume that the jet tip advances with a constant value of α equal to 2.4 for all conditions.

One can determine the jet tip celerity, in a Lagrangian sense, by differentiating the expression for the jet tip position in Eq. (1). The resulting normalized jet tip celerity is

$$\frac{\mathrm{d}X}{\mathrm{d}t}V_j^{-1} = \frac{1}{2}\alpha\left(\frac{tV_j}{d}\right)^{-\frac{1}{2}} = \frac{\alpha^2}{2}\frac{d}{X - X_0} \tag{2}$$

where time has been replaced with the expression for jet tip position. The last expression for the normalized mean celerity of the jet tip, except for the α and X_0 values, is the same as that for the centerline velocity of steady turbulent jets. Therefore, the jet tip celerity follows the same scaling as the steady jet centerline velocity. Chen and Rodi[18] suggest a value of 6.2 for the proportionality constant $\alpha^2/2$ in steady jets, whereas the reported values by Rajaratnam[19] and Wygnanski and Fiedler[20] are 6.3 and 5.7, respectively. The average of α measurements in our impulsively started jet experiments results in a value of 2.9 for $\alpha^2/2$. This value implies that the tip of the starting jet proceeds at a velocity approximately equal to one-half of the steady jet centerline velocity. The same relationship has been reported in the previous investigations of starting turbulent jets and even in the case of laminar starting jets.[5]

Reaction Length Evolution

The experiments with chemically reactive starting jets revealed that, within the extent of our tank, the core of the starting vortex remains nearly unmixed for equivalence ratios as low as 1.3, although the rest of the released fluid surrounding the core becomes mixed quite rapidly. This was expected from an earlier study of mixing in turbulent vortex rings.[21] Since small-scale mixing in the starting vortex core could not be examined in the present setup, attention was focused on the jet mixing subsequent to the separation of the starting vortex. As will be shown, the mixing within the jet at any axial location becomes equal to that in steady jets after a certain time following the passage of the jet tip.

The mean reaction length $\bar{L}$ of steady turbulent jets in aqueous media has been found to increase linearly with the reaction equivalence ratio.[10,11] The constant of proportionality was about 10. Moreover, the instantaneous reaction length oscillated quasiperiodically with a period proportional to the local jet diameter divided by the local centerline velocity.[11] The present measurements were concerned with the evolution of the instantaneous reaction length as a function of time in starting jets. At large times, the reaction length would reach an asymptotic value, associated with that in the steady jet. Dependence of the steady jet mean reaction length $\bar{L}$, normalized by the nozzle diameter, on the equivalence ratio ϕ is shown in Fig. 8. The uncertainty of the reaction length measurements is estimated to be within ±2.9 cm. The best-fit line to the data has a slope of 8.5. This is less than the previous measurements; however, the important aspect is that the mean reaction length increased linearly with the equivalence ratio.

The temporal evolution of the reaction length $L(t)$, i.e., the colored pH indicator front, for the equivalence ratio $\phi = 6.8$ at a Reynolds number of 1.5×10^4 is shown in Fig. 9. The steady-state mean reaction length $\bar{L}/d$ is denoted by the horizontal line at $63d$. The jet tip location X/d, obtained from the inert dye data in Fig. 6, and the reaction length are almost the same until $20d$, to within our experimental uncertainty. After this point, the reaction length proceeds slower than the jet tip, denoting increased mixing near the jet tip. The reaction length becomes nearly equal to the asymptotic average value of 63 nozzle diameters at about 915 nondimensional time units. At this time, the jet tip is beyond $73d$. Soon afterward, the reaction length starts to fluctuate in a manner characteristic of the steady jet. Only two oscillation cycles are apparent in this plot because the average oscillation period at this average reaction length is about 3 s, corresponding to 280 nondimensional time units. Meanwhile, the jet tip continues to extend into the ambient fluid.

If the mixing rate near the jet tip were the same as that in a steady jet, the reaction length and the jet tip would proceed at the same rate

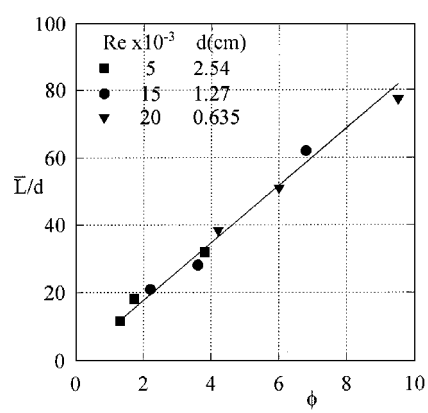

Fig. 8 Steady-state mean reaction length as a function of equivalence ratio ϕ.

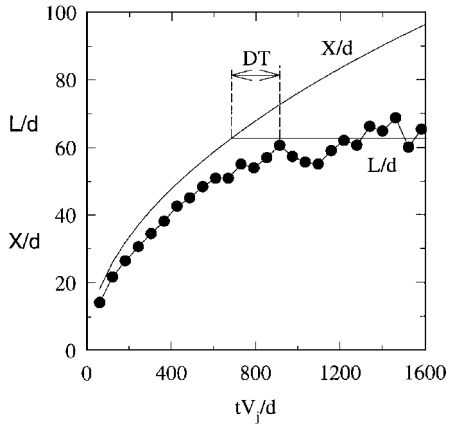

Fig. 9 Time evolution of the instantaneous reaction length *L/d* and jet tip *X/d*. The horizontal line indicates the asymptotic value of reaction length $\bar{L}$ for $\phi = 6.8$. The jet tip trajectory is taken from the inert tracer data in Fig. 6. The passage time of the region with improved mixing is denoted by ΔT.

as far as the asymptotic value. Beyond there, the reaction length would fluctuate and the jet tip would continue as before. However, the reaction length does not reach the asymptotic plateau at the same time as the jet tip, indicating that there is increased mixing near the jet tip. Once the region near the jet tip with improved mixing passes, the reaction length becomes stationary, and the jet behaves similarly to the steady jet. The extent of the region near the tip with improved mixing is argued to be proportional to the large-scale structure dimension at the location of the steady-state mean reaction length. Thus, the large structure passage time at the steady-state mean reaction length is the time period ΔT associated with faster mixing at the jet tip. The time period ΔT is defined as the time it takes the instantaneous reaction length to arrive at the steady-state mean reaction length after the jet tip has passed the same location. The time ΔT is shown graphically in Fig. 9 for the case of $\phi = 6.8$. Scaling arguments for ΔT will be presented in the next section.

Discussion

There are two major issues concerning the structure of impulsively started jets that need to be further discussed. The first is the significant difference between the normalized starting vortex separation times in the present study and those obtained in the Ref. 16. The other is the temporal and spatial scaling of the region near the jet tip with enhanced mixing. The proposed scaling is based on the jet large structures.

The issue of large differences between the present dimensionless values of vortex separation time and that of Gharib et al.[16] stems from the different methods used for characterizing the separation time. The data in Ref. 16 are based on the vortex ring circulation measurements obtained by the particle image velocimetry technique. The present visual measurements are based on the observation of pure ambient fluid in between the jet tip and the vortex ring. If the separation of vorticity occurs earlier than the appearance of ambient fluid on the centerline, then our values are expected to be larger than those in Ref. 16.

To resolve this apparent conflict, the separation time of circulation in our experiments can be estimated by calculating the time that it takes for the jet to produce an aggregate circulation equal to the vortex ring circulation.[16] The circulation produced at the nozzle is approximately equal to $V_j^2 t/2$. The vortex ring circulation at the separation point can be estimated by the product of vortex diameter $2r$ and its convective velocity U shortly after separation. Both of these values were extracted from the vortex ring spreading rate and penetration measurements. The vortex ring velocity U was found by fitting a polynomial to the ring penetration vs time data and then differentiating the polynomial to arrive at the ring velocity as a function of time. The separation time of circulation according to Ref. 16 is given by $2rU/(V_j^2/2)$. The normalized separation time would be $4(r/d)(U/V_j)$. Table 2 shows the results of these calculations.

Table 2 Normalized vortex ring radius, celerity, and separation time according to Ref. 16

d, cm	$Re \times 10^{-3}$	r/d	U/V_j	$4(r/d)(U/V_j)$
0.635	20	2.6	0.3	3.1
	12	1.5	0.4	2.4
1.27	15	1.0	1.0	4.0
	6	1.6	0.4	2.6
2.54	5	1.7	0.4	2.7

The normalized time computed in this manner is much smaller than those obtained from the visual observations. Moreover, these values with an average of 3 are quite close to that of Gharib et al. Then, the current data are consistent with those of Ref. 16 once the same definition is used for characterizing the pinch off of the starting vortex.

The extent of the enhanced mixing region near the jet tip was argued at the end of the last section to be proportional to the large-scale structure dimension at the location of the mean reaction length. If this reasoning is valid, then the first large-scale structure of the starting jet mixes faster than the rest of the jet, presumably because it encounters fresh ambient fluid all around its leading edge. The time scale T_{large} for the passage of first large-scale structure at any axial location is found by dividing the local jet width δ with the local characteristic velocity. The jet tip celerity $\mathrm{d}X/\mathrm{d}t$ was taken from Eq. (2) as the characteristic velocity,

$$T_{\text{large}} \approx \frac{\delta}{(\mathrm{d}X/\mathrm{d}t)} \sim \frac{x}{V_j[(\alpha^2/2)/(x/d)]} = \frac{2(x/d)x}{V_j\alpha^2} \qquad (3)$$

where x is the axial coordinate and the virtual origin effects have been neglected. In the preceding expression, the jet width δ was set proportional to x due to the linear spreading rate of the jet. Because the jet large-scale structures grow with the axial location, the jet region with improved mixing rate becomes larger as the jet tip travels further downstream. The time span for faster mixing ΔT, which is argued to be proportional to T_{large}, should also increase with the axial coordinate. For any equivalence ratio, the pertinent axial location is the steady-state mean reaction length, i.e., $x = \bar{L}$. Substituting this into Eq. (3) results in

$$\Delta T \sim T_{\text{large}} \sim \frac{\bar{L}^2}{V_j\alpha^2 d} \qquad (4)$$

Because the steady-state mean reaction length $\bar{L}$ is linearly proportional to the equivalence ratio ϕ (see Fig. 8), then the normalized time span during which faster mixing is observed should scale with ϕ squared,

$$\Delta T(V_j/d) \approx 11\phi^2 \qquad (5)$$

The constant of 11 was arrived at from the values for proportionality constants $\alpha \approx 2.4$, $\delta \approx 0.44x$, and $\bar{L} \approx 8.5\phi$.

To verify this line of reasoning, the time difference between the jet tip and the reaction length arrival at the steady-state mean reaction length was measured from individual time traces for each equivalence ratio. These ΔT measurements were then averaged and plotted against ϕ in Fig. 10. The ΔT values for the largest nozzle, which had the smallest equivalence ratios, are not included in this plot because the jet mixed and discolored shortly after the vortex separation. The best-fit line on the log-log plot has a slope of 1.9, and the measurements are correlated with the power law expression $6.2\phi^{1.9}$. There appears to be reasonable agreement between the proposed scaling for ΔT and the measurements despite the factor of 2 difference between the absolute values of the model and the measurements. Therefore, the large-scale structure of the jet can be used to correlate the time span of faster mixing at the jet tip with the jet parameters at any equivalence ratio. The faster mass mixing at the jet tip also implies faster momentum diffusion, which corroborates the slowing down of the jet tip in comparison with the steady jet. The first large-scale structure at the jet tip mixes mass and momentum faster than the rest of the jet in an impulsively started flow. At any axial location, the jet recovers its steady-state characteristics once this large-scale structure passes by.

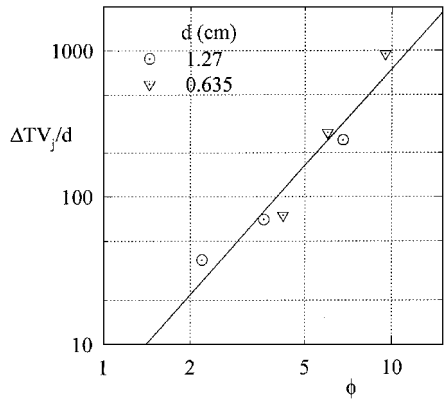

Fig. 10 Time span of faster mixing at the jet tip as a function of equivalence ratio ϕ.

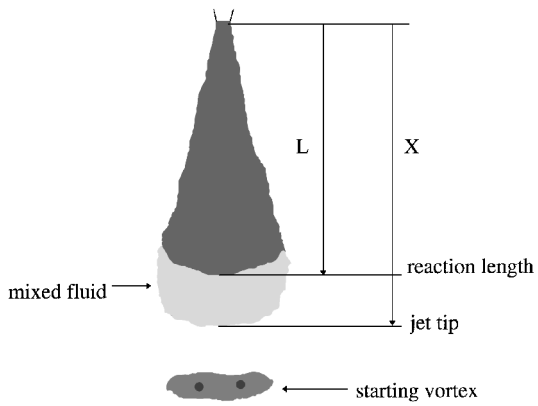

Fig. 11 Schematic structure of an impulsively started jet. The lighter shaded region at the jet tip indicates the region with faster mixing compared with the rest of the jet.

Conclusions

The impulsively started turbulent jet was investigated in a series of experiments in a water tank utilizing inert and chemically reactive markers. Based on the findings of the current study, the structure of impulsively started jets is summarized in the schematic sketch in Fig. 11. The starting vortex ring of an impulsively started jet separates from the rest of the jet in the near field after a relatively short time. As expected, the mixing in the core of the vortex ring is quite small as compared with the rest of the jet even though the released fluid surrounding the vortex mixes much faster. Beyond the very near field of the jet, the flow consists of a vortex ring that is the remnant of the starting vortex. The jet follows this vortex ring, and the distance separating the vortex ring from the jet tip increases with time due to the difference in the entrainment rates of the jet and the vortex ring. The jet tip proceeds downstream at a rate proportional to the square root of the dimensionless time. The jet tip celerity, found from the derivative of the penetration data, is approximately one-half of the centerline velocity of a steady jet, with the same nozzle exit conditions, at the same location. The jet tip follows the same scaling as the steady jet.

Results of the chemically reactive experiments reveal that the jet tip mixes with the ambient faster than the rest of the jet. The extent of the region near the jet tip with improved mixing increases with the downstream distance and is shown to be proportional to the large-scale structure at the jet tip. The axial extent of this region is approximately one-half of the local jet width or one-half of the local large-scale structure length. This was inferred from the time ΔT associated with improved mixing being half as much as the time for passage of the large-scale structure at the jet tip. Thus the unsteady effects are primarily confined to this jet region immediately upstream of the jet tip, at least as far as mass mixing is concerned. The proximity of pure ambient fluid to the jet tip region and the process of vortex separation are possible reasons for improved mixing near the jet tip. Further work is needed to elucidate the mechanism for the increased mixing and the details of the concentration field near the jet tip.

Acknowledgments

Support of this project by the National Science Foundation Grant CTS-9309321 is gratefully acknowledged. Ken Desabrais' help with the processing of starting vortex separation time is greatly appreciated. Discussions with M. Gharib regarding the separation of vorticity in starting jets were quite beneficial.

References

[1]Bradshaw, P., Ferris, D. H., and Johnson, R. F., "Turbulence in the Noise-Producing Region of a Circular Jet," *Journal of Fluid Mechanics*, Vol. 19, Pt. 4, 1964, pp. 591–624.

[2]Crow, S. C., and Champagne, F. H., "Orderly Structure in Jet Turbulence," *Journal of Fluid Mechanics*, Vol. 48, Pt. 3, 1971, pp. 547–591.

[3]Bremhorst, K., and Hollis, P. G., "Velocity Field of an Axisymmetrically Pulsed, Subsonic Air Jet," *AIAA Journal*, Vol. 28, No. 12, 1990, pp. 2043–2049.

[4]Cantwell, B. J., "Viscous Starting Jets," *Journal of Fluid Mechanics*, Vol. 173, 1986, pp. 159–189.

[5]Abramovich, S., and Solan, A., "The Initial Development of a Submerged Laminar Round Jet," *Journal of Fluid Mechanics*, Vol. 59, Pt. 4, 1973, pp. 791–801.

[6]Kuo, T.-W., Syed, S. A., and Bracco, F. V., "Scaling of Impulsively Started, Incompressible, Laminar Round Jets and Pipe Flows," *AIAA Journal*, Vol. 24, No. 3, 1986, pp. 424–428.

[7]Witze, P. O., "The Impulsively Started Incompressible Turbulent Jet," Sandia National Labs., Rept. SAND80-8617, Livermore, CA, Oct. 1980.

[8]Turner, J. S., "The 'Starting Plume' in Neutral Surroundings," *Journal of Fluid Mechanics*, Vol. 13, Pt. 3, 1962, pp. 356–368.

[9]Lahbabi, F. Z., Boree, J., Nuglisch, H. J., and Charnay, G., "Analysis of Starting and Steady Turbulent Jets by Image Processing Techniques," *Third Symposium on Experimental and Numerical Flow Visualization*, FED-Vol. 172, American Society of Mechanical Engineers, New York, 1993, pp. 315–321.

[10]Weddell, D. S., "Turbulent Mixing in Gas Flames," Ph.D. Thesis, Chemical Engineering Dept., Massachusetts Inst. of Technology, Cambridge, MA, 1941.

[11]Dahm, W. J. A., and Dimotakis, P. E., "Measurements of Entrainment and Mixing in Turbulent Jets," *AIAA Journal*, Vol. 25, No. 9, 1987, pp. 1216–1223.

[12]Breidenthal, R. E., "Structure in Turbulent Mixing Layers and Wakes Using a Chemical Reaction," *Journal of Fluid Mechanics*, Vol. 109, 1981, pp. 1–24.

[13]Maxworthy, T., "Some Experimental Studies of Vortex Rings," *Journal of Fluid Mechanics*, Vol. 81, Pt. 3, 1977, pp. 465–495.

[14]Higuchi, H., Anderson, R. W., and Zhang, J., "Three-Dimensional Wake Formations Behind a Family of Regular Polygonal Plates," *AIAA Journal*, Vol. 34, No. 6, 1996, pp. 1138–1145.

[15]Koochesfahani, M. M., and Smiljanovski, V., "Initial Acceleration Effects on Flow Evolution Around Airfoils Pitching to High Angles of Attack," *AIAA Journal*, Vol. 31, No. 8, 1993, pp. 1529–1531.

[16]Gharib, M., Rambod, E., Dabiri, D., Hammache, M., Shiota, T., and Sahn, D., "Pulsatile Heart Flow: A Universal Time Scale," *Proceedings of the Second International Conference on Experimental Fluid Mechanics*, Levrotto and Bella, Torino, Italy, 1994, pp. 34–39; see also "A Universal Time Scale for the Formation of Vortex Rings," *Bulletin of the American Physical Society*, Vol. 40, No. 12, 1995, p. 1920.

[17]Kouros, H., Medina, R., and Johari, H., "Spreading Rate of an Unsteady Turbulent Jet," *AIAA Journal*, Vol. 31, No. 8, 1993, pp. 1524–1526.

[18]Chen, C. J., and Rodi, W., *Vertical Turbulent Buoyant Jets*, Pergamon, New York, 1980.

[19]Rajaratnam, N., *Turbulent Jets*, Elsevier, Amsterdam, 1976, p. 48.

[20]Wygnanski, I., and Fiedler, H., "Some Measurements in the Self-Preserving Jet," *Journal of Fluid Mechanics*, Vol. 38, Pt. 3, 1969, pp. 577–612.

[21]Johari, H., "Chemically Reactive Turbulent Vortex Rings," *Physics of Fluids*, Vol. 7, No. 10, 1995, pp. 2420–2427.

F. W. Chambers
Associate Editor